King Saud University

Arabian Journal of Chemistry

www.ksu.edu.sa
www.sciencedirect.com

ORIGINAL ARTICLE

Acylhydrazone-modified guar gum material for the highly effective removal of oily sewage

Junchi Ma [a,b], Yanru Gu [a,b], Depeng Ma [a,b], Weizhao Lu [a,b], Jianfeng Qiu [a,b,*]

[a] *Translational medicine research centre, The First Affiliated Hospital of Shandong First Medical University & Shandong Provincial Qianfoshan Hospital, Jinan, Shandong, China*
[b] *School of Radiology, Shandong First Medical University & Shandong Academy of Medical Sciences, Jinan, Shandong, China*

Abstract   Oily sewage poses a serious environmental risk normally; thus, herein, the modified guar gum (GG-SH) was prepared through rapid condensation reaction between polysaccharide and stearic hydrazide. GG-SH exhibited high removal efficiency of crude oil, the maximum adsorption capacity was calculated to be 2157.3 mg•g-1. The kinetics and isotherm statistical theories showed that the sorption of crude oil onto GG-SH was governed by pseudo-second-order, and Langmuir models, respectively. The removal rate was still high after six cycles of regeneration, indicating an outstanding technique to prepare polysaccharide-based material for the oily sewage treatment with high efficiency and recyclability.

1. Introduction

Frequent oil spill accidents and water pollution caused by industrial oil wastewater discharge seriously threaten the marine ecological environment and human health (Cheng et al., 2020, Asadu et al., 2021, Black et al., 2021, Chhabra and Singh 2021, Ding et al., 2021, Damavandi and Soares 2022). Approximately 10 billion m³ of oily wastewater is produced worldwide every year according to statistics, and this amount still continues to increase(Bajpai et al., 2020). Emulsified oil are quite complicated compounds that are usually composed of conjugated phenyl structures, which are responsible for their non-

degradability and high toxicity(Baloo et al., 2021, Gkogkou et al., 2021, Guselnikova et al., 2021, Haselroth et al., 2021, He et al., 2022). Hence, oily sewage and sludge are heavy burdens for economy and environment(Liu et al., 2018, Ge et al., 2019, Tan et al., 2022). Due to the fact most components on this type have very low biodegradability, they are stable toward heat, light, and oxidizing agents their liberation to the environment through wastewaters may affect the biosphere(Kilany et al., 2020, Jiat Lee et al., 2021, Kallem et al., 2021, Kirkebæk et al., 2021, Krebsz et al., 2021, Lawal et al., 2021, Magalhães et al., 2021, Mahdi et al., 2021). In addition, they are mutagenic and carcinogenic. In this circumstance, several methods can be applied for detection and treatment of wasterwater(Yamini et al., 2012, Abdel Maksoud et al., 2020, Tang et al., 2020, Guan et al., 2021, Osman et al., 2022, Tawfik et al., 2022)., including chemical precipitation, demulsification, oxidation process(Tawfik et al., 2022), adsorption(Bai et al., 2022), degradation(Liu et al., 2022) and photocatalysis(Shamloufard et al., 2022, Wang et al., 2022). Of these methods, adsorption is most widely used owing to its advantages of cheap, efficient and easy to use. There are various raw materials used for oil adsorption, such as supramolecular gels(Medina et al., 2021,

ELSEVIER | **Production and hosting by Elsevier**

Mottaghi et al., 2021, Shui et al., 2021), carbon-based materials(Gupta et al., 2014, Diraki et al., 2019, Yang et al., 2019, Schaefer et al., 2021, Shi et al., 2021, Yang et al., 2021, Zhang et al., 2021), silicon material (Li et al., 2018), metallic nanoparticles(Al-Husaini et al., 2019, Alheety et al., 2019, Bi et al., 2019, El-Maghrabi et al., 2019, Javadian et al., 2019, Elmobarak and Almomani 2021, Farahbod and Afkhami Karaei 2021, Kallem et al., 2021, Damavandi and Soares 2022), zeolitic imidazolate frameworks(Ahmadi et al., 2021, Ahmadi et al., 2022, Naeini et al., 2022, Naeini et al., 2022), metal oxides(He et al., 2022) and 3D imprinted polymers(Arabi et al., 2016, Arabi et al., 2017, Ostovan et al., 2018, Bagheri et al., 2019). However, these adsorbents still have some drawbacks, such as either low or limited adsorption capacities or poor extraction efficiencies(Liu et al., 2014). Moreover, most of them are problematic in terms of their recycling and reuse. The criteria for the selection of ideal adsorbents are based on several factors that include effective, safe, eco-friendly, low-cost recyclability, high porosity, adsorbent cost and easiness in separation(Abdel Maksoud et al., 2020, Osman et al., 2022). Therefore, novel high-efficiency adsorbents still need to be studied and created.

Among all those adsorbents reported before, bio-based materials have drawn much attention for trapping analytes in recent years(Sun et al., 2008, Ahmaruzzaman and Gupta 2011, Al.Haddabi et al., 2015, Chai et al., 2015, El Shahawy and Heikal 2018, Phanthong et al., 2018, Bao et al., 2019, Li et al., 2020, Martins et al., 2020, Zhang et al., 2020, Zhang et al., 2021). Polysaccharide was famous for its low cost, clean and reactivity. Guar gum is a kind of chained polysaccharide, which has attracted special attention due to its availability, low cost and environmental protection characteristics. In addition, their surfaces can be easily customized to meet functional. Despite the fact that guar gum and its derivatives have broad variety of applications, they suffer from drawbacks like high hydrophilic and swelling characters(Chandrika et al., 2016, Yang et al., 2017). Chemical modification of guar gum is indeed an efficient way not only for circumventing the drawbacks of the polysaccharide, but also for improving its properties and those of grafted functional groups (Patra et al., 2017). A number of efforts have been undertaken to develop modified gum-based adsorbents with their desired properties at present(El Assimi et al., 2019, Wang et al., 2019, Saya et al., 2021, Tabatabaeian et al., 2021). When referring to how to produce high-efficiency adsorbent, it mentioned mainly process changes and the use of modification of carbohydrate chain(Mukherjee et al., 2018, Gihar et al., 2021, Saya et al., 2021).

Previous studies have found a series of highly effective adsorbents based on modified guar gum for dealing with toxic waterborne contaminants(Duan et al., 2019, Ma et al., 2019). Herein, our purpose is to optimize properties of guar gum with simple procedures in order to develop new and efficient adsorption materials for the treatment of oily sewage. Binding with stearyl hydrazine enhances the surface area of the polymer matrix and provides additional binding sites for more efficient adsorption of contaminants. The adsorption properties of stearic acylhydrazone modified guar gum (GG-SH) for crude oil in aqueous solution were examined. The material exhibited dramatic capacity of demulsification and separation for oily sewage. The exceptionally high adsorption capacity of the GG-SH in the uptake of oil was explained on the basis of different structural and morphological characterization results.

2. Experimental

2.1. Materials

Guar gum was purchased from Aladdian Inc(viscosity: 5000 mPa.s; 200 mesh). Ethanol (99.0 % purity), p-toluenesulfonic acid monohydrate(TsOH) (98 % purity), ethyl stearate (98 % purity), KBr (99 % purity), hydrazine monohydrate (80 % purity) were purchased from Adamas Inc and used

without further purification. Oily sewage was obtained from oilfield in the Bohai Sea.

2.2. Preparation

2.2.1. Synthesis of stearic hydrazide

3.12 g (10 mmol) ethyl stearate, 10 mL hydrazide hydrate (80 %) and 50 mL ethanol were placed in a 250 mL flask and stirred until completely dissolved. The system was stirred at 78 ℃ and refluxed for 4 h. The solution was cooled to room temperature to obtain white flocculent crystals, which were filtered and recrystallized with 50 % ethanol aqueous solution.

2.2.2. Preparation of stearic acylhydrazone modified guar gum (GG-SH)

AGG (Dialdehyde guar gum) was prepared via a literature method (Duan et al., 2019), and was ultrasonic dispersed in ethanol for 30 min. A mixture of AGG (2 g), stearic hydrazide (3.2 g) and TsOH (0.5 g) were stirred at 45 °C for 72 h while white powder was obtained, filtered and washed with ethanol for three times to remove excess stearic hydrazide and catalyst. The products were dried in a vacuum oven at 45℃ for 12 h. The detailed preparation procedure of GG-SH was described in the Supporting Information (Figure S1).

2.3. Characterization

Fourier Transform infrared spectrometer (FT-IR-S-8400) used KBr disk for FT-IR spectral analysis in 400–4000 cm^{-1} region. Scanning electron microscope (SEM) images were obtained on a field emission scanning electron microscope (SU8220). Optical microscope images were obtained by laser scanning confocal microscope (LSCM, Eclipse Ti, Nikon, Japan) with excitation wavelength of 488 nm.

2.4. Experimental methods

The oil content of sewage is an important index to evaluate the properties of oil absorbing materials in this paper, according to the UV-fluorescence spectrophotometry, using OilTech121A handheld oil measuring instrument to determine the oil content in sewage, the operation steps are as follows:

(1) Remove 100 μL dehydrated crude oil with a pipette gun into a 100 mL volumetric flask, add n-hexane to dissolve it, and set the volume to 1000 mg/L standard crude oil solution.

(2) Dilute the standard crude oil solution with n-hexane to six concentration gradients of 10 mg/L, 25 mg/L, 50 mg/L, 100 mg/L, 250 mg/L and 500 mg/L, respectively.

(3) Add the prepared solution into the sample tube and calibrate the instrument.

(4) Take a quantitative amount of oil-bearing sewage, extract the crude oil with n-hexane, take the oil phase of the upper layer and dilute it with n-hexane again for ten times to prevent the measured value from exceeding the instrument range, use an oil meter to measure the oil content in oil-bearing sewage before and after treatment, and record it as X1 and X2 respectively. Formula is used to calculate the oil removal rate of the process.
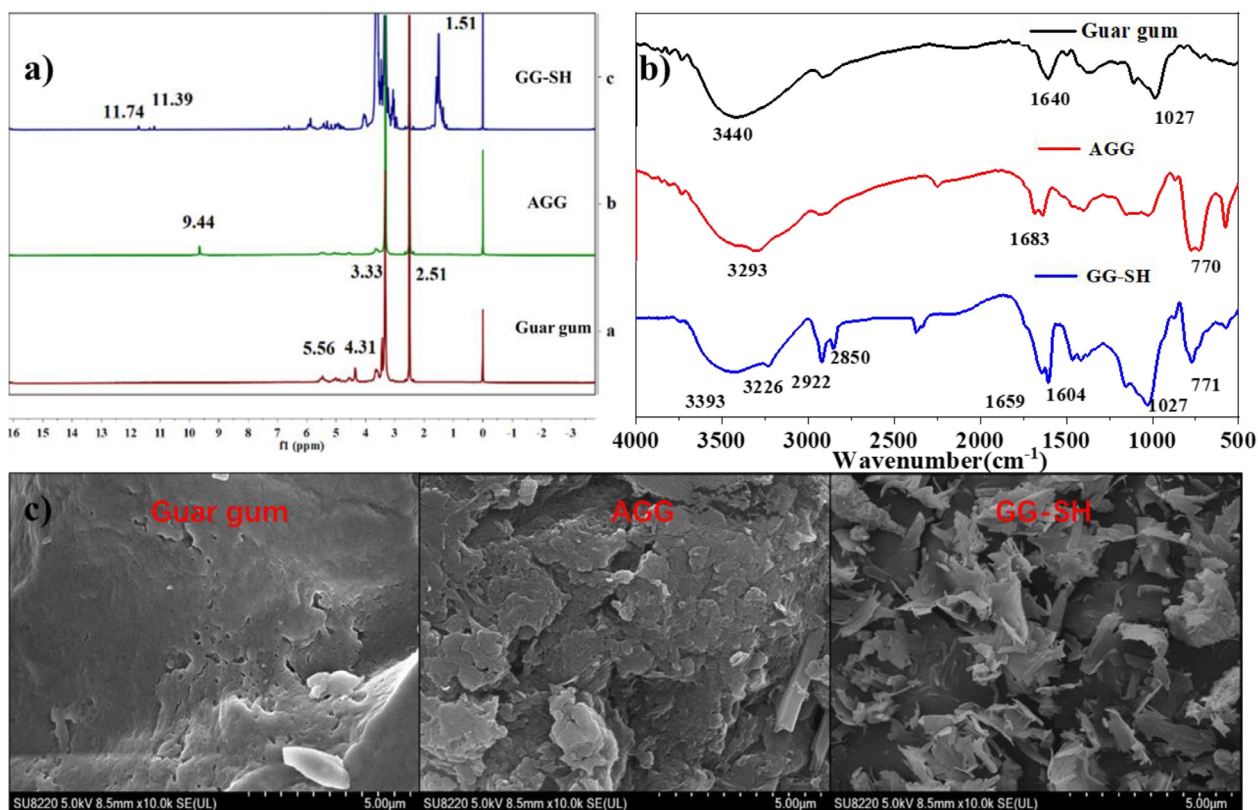
$$\alpha = \frac{x_1 - x_2}{x_1}$$

Fig. 1 A)^{1}H NMR spectra of guar gum, AGG and GG-SH; b)FT-IR Spectra of guar gum, AGG and GG-SH. c) SEM images of guar gum, AGG and GG-SH.

Where: α = oil removal rate, %.

X_1 = Oil content of sewage before treatment, mg/L.

X_2 = Oil content of treated sewage, mg/L.

For the desorption experiment, the emulsified oil adsorbed GG-SH were washed thoroughly with ethanol. After desorp-

tion equilibrium, the adsorbent was reused in adsorption experiments (adsorbent, 5 mg; oily sewage, 10 mL) and the process was repeated six times.

3. Results and discussion

3.1. Characterization

3.1.1. ^1H NMR

^{1}H NMR spectra of natural guar gum, AGG and GG-SH are shown in Fig. 1 a) below, respectively. By comparing the spectra of the three, the peaks appearing at 4.5–5.5 ppm are attributed to in the –OH group in the mannose and galactose. The
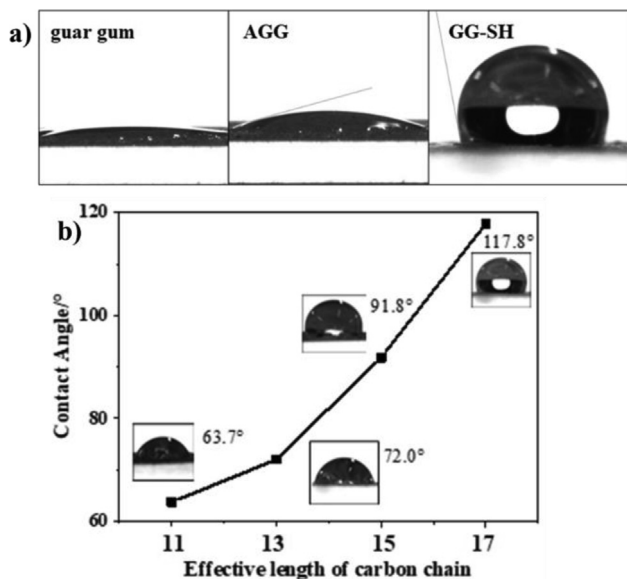

Fig. 2 A) contact angle of guar gum, agg and gg-sh; b) contact angle of a series of different long chain alkylhydrazone modified guar gum.
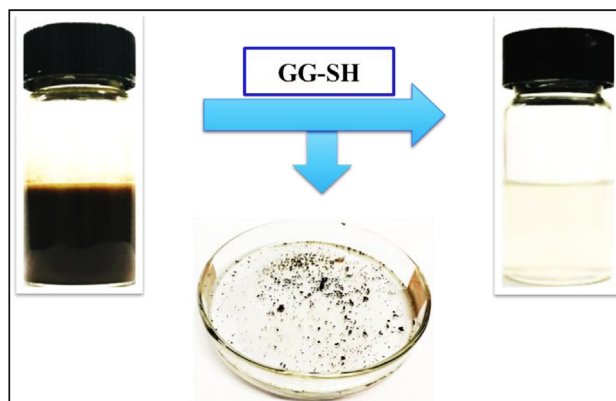

Fig. 3 Oil removal performance of GG-SH.

peak appearing at 9.44 ppm is attributed to the aldehyde group in the structure of AGG, showing that AGG was prepared via oxidation using sodium periodate. As is displayed in the spectra of GG-SH, the multiple peaks in 1.51 ppm are attributed to the long main chain of alkyl groups, demonstrating the modification of AGG with stearic hydrazide has achieved. ^{1}H NMR spectra confirmed that non-aqueous long chain alkane was partially grafted on structures of polysaccharides.
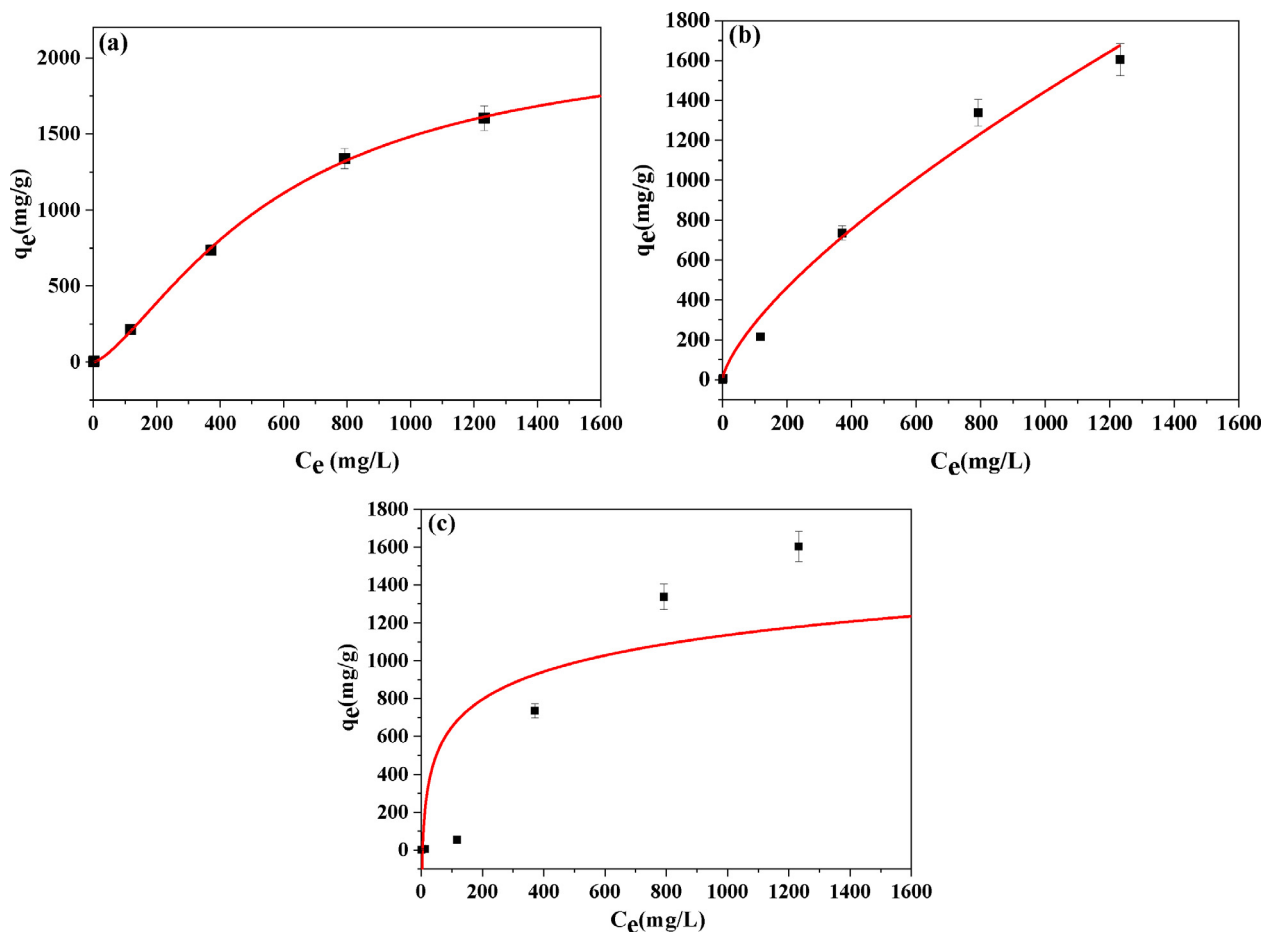

Fig. 4   (a) Langmuir, (b) Freundlich, and (c) Temkin isotherms for the adsorption of oily sewage by GG-SH.
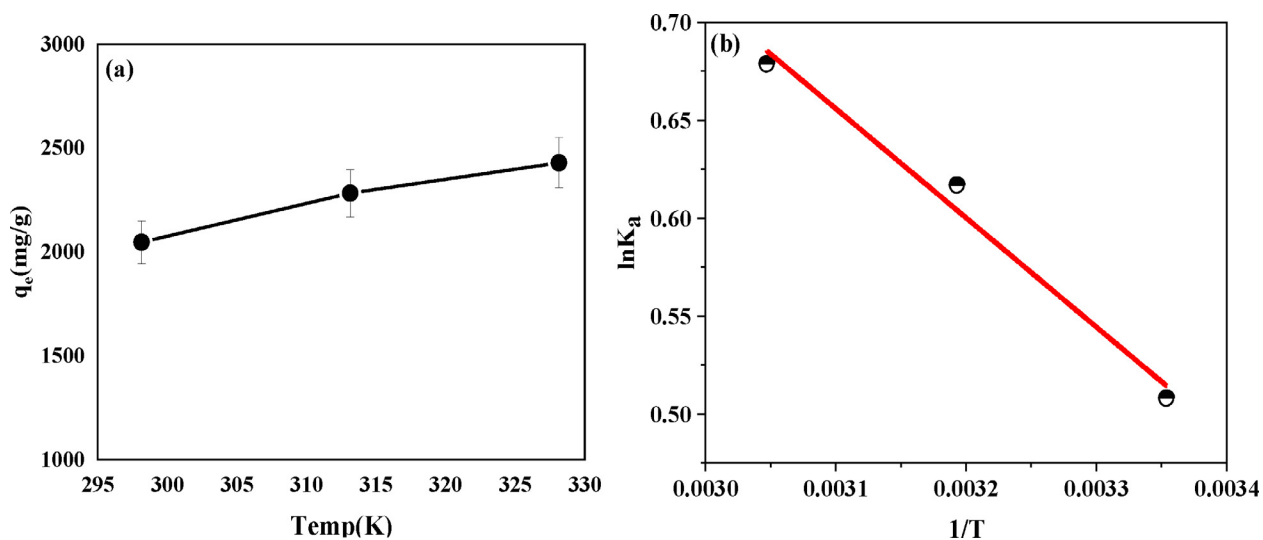

Fig. 5   (a)The adsorption capacity of GG-SH at 298.15 K, 313.15 K and 328.15 K; (b)The adsorption thermodynamics curve of oil adsorption by GG-SH.

3.1.2. FT-IR

To further investigate the structure of GG-SH, an FT-IR study was carried out (Fig. 1b). In the spectra of guar gum, the absorption peaks at 3430 cm^{-1}, 2931 cm^{-1} belongs to the –OH group, and C—H stretching vibrations, respectively. In the spectra of AGG, the peak appearing at 1698 cm^{-1} is attributed to the C=O, indicating the successful oxidation of sodium periodate. As is shown in spectrum of GG-SH, the peaks at 2922 cm^{-1} and 2850 cm^{-1} are attributed to methylene on the long chain alkyl group, showing the condensation of AGG with stearic hydrazide has achieved.

3.1.3. SEM

The microstructures of GG-SH were manifested from their SEM images. Fig. 1c are representative SEM images of guar gum, AGG and GG-SH, respectively. Modified material GG-SH particle surface has a large number of chaotic flake stack structure and accompanied by a large number of hollow spaces(Wen et al., 2021). The appearance of the structure differences might be due to the introduction of the long alkyl chain increases the modification of the van der Waals force of guar gum, make it to a certain extent, shows the tendency of 3 d mesh, and further increase the material's surface area. This provides structural and theoretical basis for the subsequent study on the treatment performance of modified guar gum to oil pollutants.

3.1.4. Static contact angle experiments

Static contact angle experiments are widely used to demonstrate the hygroscopicity of solid surfaces in contact with liquids. Therefore, after oxidation modification, the hydroxyl group in the structure of the aldehyde guar gum is transformed into aldehyde group, and the difference of hydrophilicity between long chain alkyl, aldehyde group and hydroxyl group results in the significant contact angle change of guar gum, AGG and GG-SH. Fig. 2a showed the contact angle values
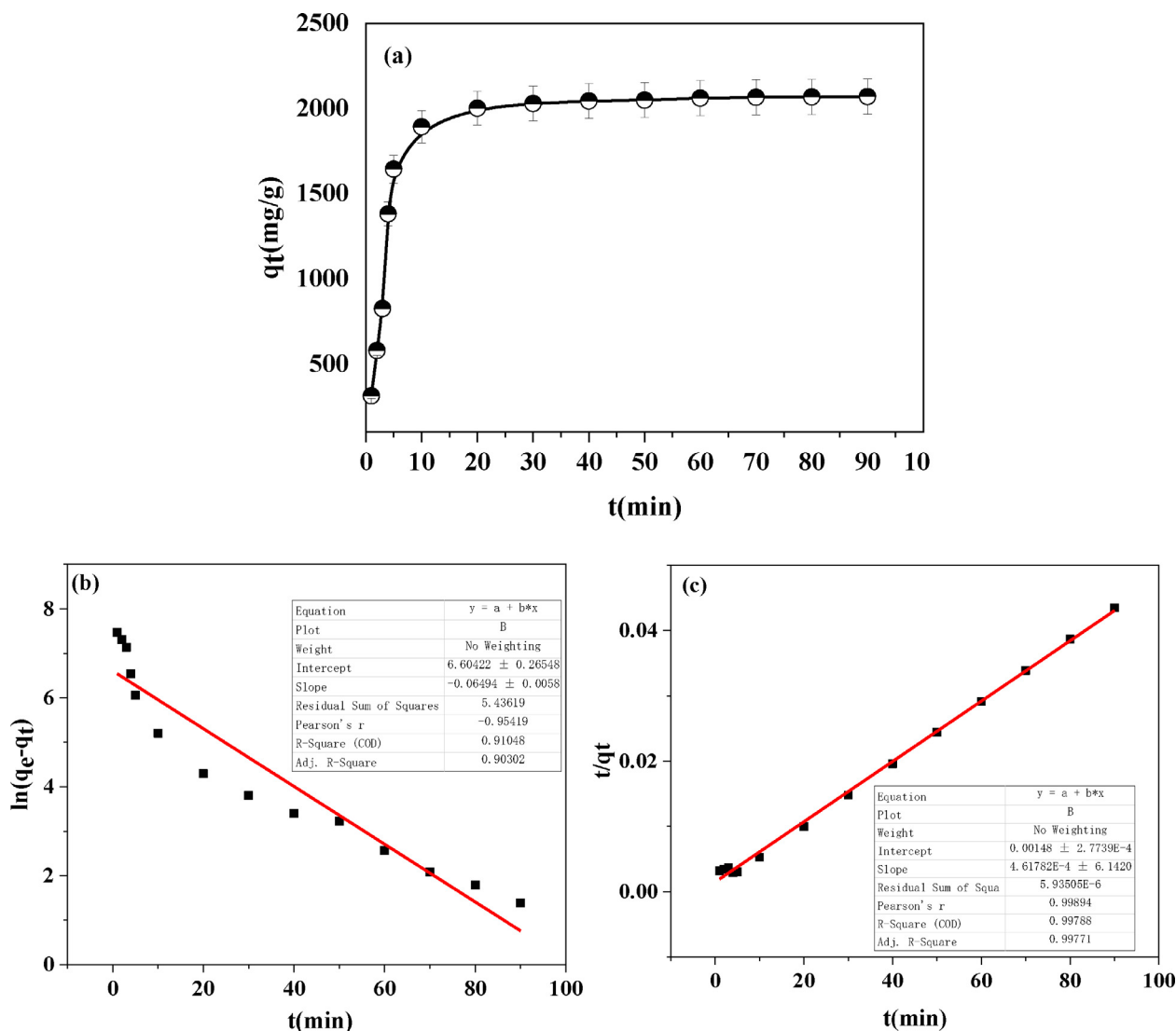

Fig. 6 A) the adsorption capacity of gg-sh in different adsorption time; b) pseudo-first-order kinetic plots for oil adsorption onto gg-sh; c) pseudo-second-order kinetic plots for oil adsorption onto gg-sh.

of guar gum, AGG and GG-SH. The glue droplets of stearyl acylhydrazone modified by long chain alkyl can exist stably on the surface of the sample without wetting, and the contact angle with water is 117.8°. The contact angle results show that the introduction of alkyl can effectively improve the surface tension between carbohydrate and water, and improve the hydrophobicity of the target material. Polysaccharides are polar groups and alkyl groups are non-polar groups, introduction of stearyl substituent not only improves the affinity of the adsorbent to oil making it easier to capture oil droplets, but also reduce the polarity to prevent the adsorbent from reuniting.

In order to explore the relationship between the length of alkyl and hydrophobicity of modified guar gum, a series of hydrazides with different carbon chain lengths were selected to be combined with AGG, and corresponding alkylhydrazone modified guar gum were prepared according to preparation section. The relationship between hydrophobicity and carbon chain length was determined by the contact angle test with water as shown in Fig. 2b. The experimental results showed that the hydrophilicity of the modified guar gum decreases and the contact angle increases with the increasing of the carbon chain.

3.1.5. BET analysis

Nitrogen gas sorption isotherms at 77.35 K corresponded to the calculated specific surface area BET in Figure S4. The average pore size distribution of GG-SH calculated based on Barret-Joyner-Halenda theory(Shi et al., 2022) (BJH) was found to be 1.753 nm, which can offer high accessibility to adsorption sites. BET surface area was calculated to 4.437 m^2/g. After adsorption, BET surface area was decreased to 0.952 m^2/g due to the occupancy of adsorption site by oil components.

3.2. Adsorption study

In order to study the adsorption performance of GG-SH towards oil components the oily sewage from an oilfield in Bohai Sea was selected as the treatment object. Adding 0.1 g GG-SH powder to 20 mL oily wastewater, shake for 10 min to make it completely mixed and then stand for 15 min, the color change of water sample will be observed. Fig. 3 shows the comparison of oily sewage before and after the treatment. Apparently, GG-SH has a significant adsorption effect on emulsified oil components in sewage, and the treated water is clear and nearly colorless, confirming that GG-SH is an efficient oil adsorption material.(See Fig. 4).

3.2.1. Adsorption isotherms

Interaction of solid–liquid phase during the adsorption process would be explained by the adsorption isotherm. Different types of models, like Langmuir, Freundlich and Temkin isotherm(Liu et al., 2021), were applied to simulate and understand the adsorption mechanism of crude oil on GG-SH. On the basis of the results in Fig. 6, the adsorption isotherms may follow the Langmuir model, the experimental values of q_m for oily sewage was calculated to be 2157.3 mg•g^{-1}(-

Table 1 Adsorption capacities of various adsorbents for the adsorption of oily sewage.

Adsorbents	Adsorption time (h)	Maximum adsorption capacities (mg/g)	recycle	Refs
Stearic acylhydrazone modified guar gum	0.1	2157.3	6	This work
Amphiphilic Chitosan Derivative	0.1	714.4	3	(Sun et al., 2008)
Surfactant modified sepiolite	1.5	454.6	5	(Li et al., 2018)
GO powder	0.2	1335.1	3	(Diraki et al., 2019)
Phragmites australis	2.0	3333.5	3	(El Shahawy and Heikal 2018)
Ultra-light carbon foams	1.5	1627.8	–	(Yang et al., 2019)
Modified date seeds	2.0	74.6	–	(Al.Haddabi et al., 2015)

Table 2 Adsorption kinetics of various adsorbents for the adsorption of oily sewage.

Adsorbents	Adsorption time (h)	Kinetic models	R^2	Refs
Stearic acylhydrazone modified guar gum	0.1	Pseudo-second-order	0.997	This work
Modified diatomaceous earth	0.83	Pseudo-second-order	0.999	(Sakti et al., 2022)
Polyether polysiloxane-grafted ZIF-8	1.5	Pseudo-first order	0.996	(Wu et al., 2021)
Magnetic hollow buoyant alginate beads	1	pseudo-second order	0.999	(Sakti et al., 2021)
Hyperbranched polyglycerol polymer-coated silica nanoparticles	0.5	pseudo-second-order	0.997	(Elmobarak and Almomani 2021)
Stearic acid grafted mango seed shell	0.67	Bahattacharya-Venkobachor order	0.994	(Asadu et al., 2021)
Stearic acid grafted coconut husk	0.8	pseudo-second-order	0.997	(Asadu et al., 2021)
Modified pinewood biochar	1.0	Pseudo-first order	0.986	(Gurav et al., 2021)

3.2.2. Adsorption thermodynamics study

To explore the effect of temperature on the oil removal rate of GG-SH, thermodynamics experiments were designed and performed. Fig. 5 showed the experimental data of the adsorption performance of GG-SH on oily sewage at 298.15 K, 313.15 K and 328.15 K. The thermodynamic data analysis diagram is obtained by plotting with 1/T as abscess and lnK_a as ordinate. Table S2 shows the thermodynamic parameters during adsorption at different temperatures calculated by Van't Hoff equation formula.

ΔG^θ is always negative in the process of GG-SH adsorption on oily sewage, which proves that the adsorption of oil components by GG-SH is a spontaneous process(Liu et al., 2021). ΔH^θ is 4.64 kJ/mol, which indicates that the adsorption process is endothermic, the increase of temperature is beneficial to the adsorption process within a certain temperature range(Li et al., 2021, Wen et al., 2021). The speculated reason is that with the increase of temperature, the molecular motion increases, and the non-polar oil component can more quickly combine with the GG-SH, so as to achieve better adsorption effect. ΔS is 19.83 J/(mol·K), confirming that DOF(degree of freedom) of adsorption process increases. The oily sewage in the oil composition including alkane and aromatic hydrocarbon, compared with the water molecules to its large volume, GG-SH surface adsorption of oil droplets and at the same time with the stripping of several water molecules. In this case, the entropy increase caused by water molecule desorption may greatly exceed the entropy decrease caused by oil droplet adsorption, so the DOF increases in the whole system adsorption process.

3.2.3. Adsorption kinetics study

The influence of time on the adsorption performance of GG-SH on oily sewage was discussed. Fig. 6a shows the adsorption amount of GG-SH with the change of adsorption time within 90 min. As shown in Fig. 6, within 10 min after the adsorption, the adsorption rate of GG-SH on oil components was relatively fast, the adsorption amount increased and the adsorption equilibrium could be basically achieved. The reason is that in the early stage of adsorption, the concentration of oil components in sewage is higher, and the oil droplets gather faster on the surface of the adsorbent, so the adsorption rate is higher. After 30 min, the adsorption capacity basically did not increase and reached the adsorption equilibrium state.

The kinetic fitting curve of GG-SH adsorption of oil components in oily wastewater is shown in Fig. 6b and 6c. Experimental results show that the adsorption process is fast in 10 min and reaches the adsorption equilibrium after 30 min. As can be seen from the fitting results of the kinetic equation in Table S3, the Pseudo-first-order kinetic plots has poor fitting results for the kinetic data of the adsorption process, and the correlation parameter R^2 is only 0.903, while the Pseudo-second-order model is in good agreement with the kinetic data of the adsorption process(Li et al., 2019, Shi et al., 2022), and the correlation parameter R^2 can reach 0.997. The calculated value of adsorption capacity obtained by formula fitting is also close to the experimental value. Adsorption kinetics of various adsorbents for the adsorption of oily sewage was shown in Table 2 below.
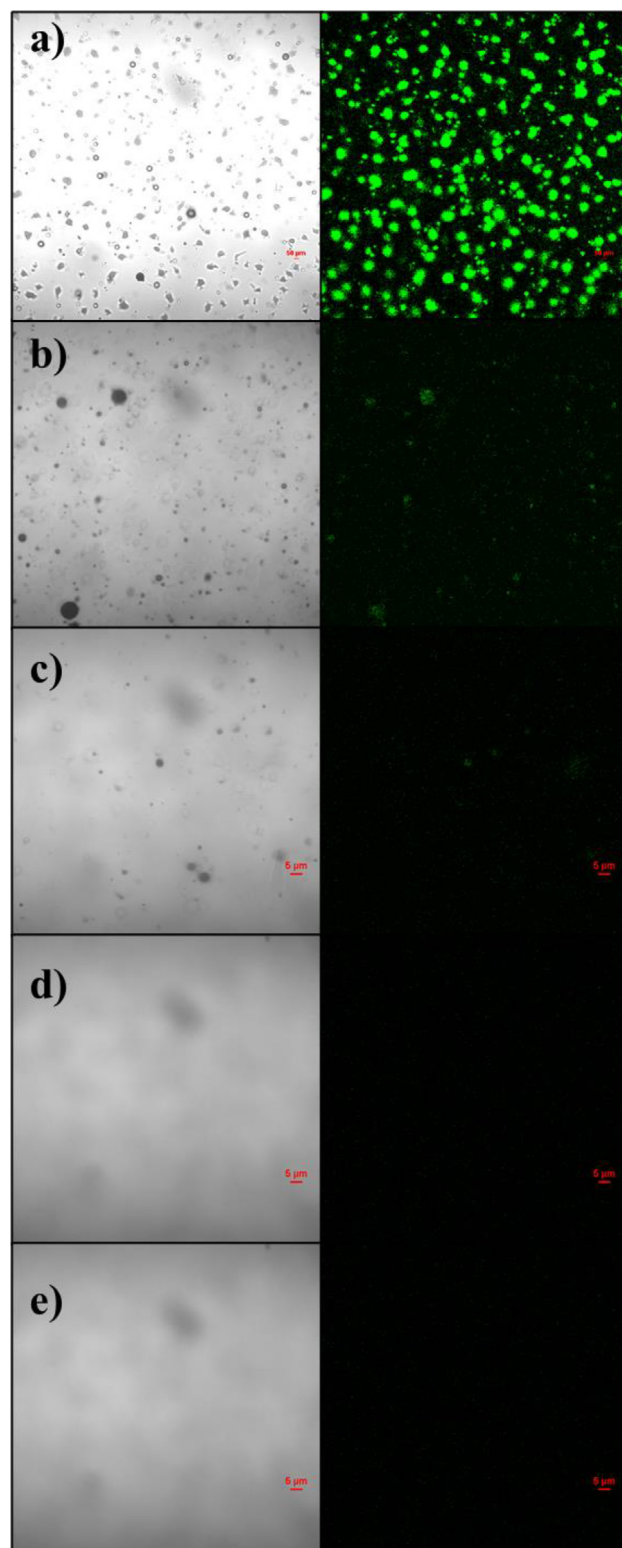
Table S1). It is important to note that, as shown in Table 1, the maximum adsorption capacity is much higher than previously reported values for adsorbents.

Fig. 7 Confocal fluorescence microscopy of oily sewage treating with different amount of GG-SH. a)0 mg; b)50 mg; c)100 mg; d) 150 mg; e)200 mg.(λ = 488 nm).

3.3. Laser confocal fluorescence microscopy

To more intuitively understand the content changes of oil components before and after GG-SH treatment of sewage, confo-

cal fluorescence microscope was used in this experiment to observe the fluorescence imaging of oily sewage under UV light. Through the fluorescence imaging of oil components, the adsorption performance of GG SH was further explained.

As can be seen from Fig. 7a, a large number of oil droplets in the liquid phase can be clearly seen in the bright field of the oily sewage before treatment, and the fluorescence images under the excitation of UV light also show the existence of a large number of phosphor dots, indicating the existence of conjugated luminescent group structures in the sewage. With the assistance of GG-SH, the oil droplets in the liquid phase were gradually separated from the water. Therefore, it can be seen from Fig. 7b that the fluorescence points in the image were significantly reduced, confirming that oil droplets had been removed. When the amount of GG-SH added to the system is 200 mg, as shown in Fig. 7e, no oil droplets can be observed in the brightfield, and there are basically no fluorescent points, demonstrating that the oil components in sewage have been basically removed completely.

Figure S5 shows confocal microscope images of GG-SH adsorbent before and after adsorption. From Figure S3 a, it can be seen that GG-SH is granular in the brightfield and is non-fluorescent even under excitation of UV light. After adsorption, it was obvious in Fig. S3b that adsorbent was covered with a large number of oil components. Fluorescence images also confirmed that oil had been transferred from the water phase to the surface of adsorbent by GG-SH.

3.4. Adsorption-desorption studies

In practical application, the recycling performance of oil-absorbing materials is of great importance. Therefore, in order to investigate the recycling performance of GG-SH as a novel oil adsorbent, adsorption–desorption experiments of the adsorbed oil from the GG-SH were conducted. As can be seen from Fig. 8, when GG SH package is placed in sewage, the water phase gradually became clarified, and the non-polar oil components in sewage were adsorbed into the package by the intermolecular association force with the long chain alkyl group on GG-SH. The treated water sample wrapped with GG-SH was taken out for oil content determination and the experiment was repeated. In each subsequent cycle, the amount of adsorption decreases slowly due to incomplete desorption of oil, but GG-SH can still be reused to removel oil from an aqueous solution and still have good performance (Fig. 8c).

3.5. Adsorption mechanism

For the purpose of analysing the intermolecular force in the oil-absorbing process, the IR spectra of GG-SH before and after adsorption were performed and compared, and the results were shown in the figure below. As shown in Fig. 8, the absorption peak of hydroxyl in GG-SH appeared at 3393 cm^{-1}, and the corresponding absorption peak in infrared spectrum of GG-SH powder at the late stage of adsorption appeared at 3383 cm^{-1}. The carbonyl peak of the functional group of the acylhydrazone also moved from 1659 cm^{-1} to 1639 cm^{-1}, indicating that hydroxyl and hydrazone groups were involved in hydrogen bond formation. In addition, asymmetric and symmetric stretching vibration peaks of $-CH_2$- appeared at 2922 cm^{-1} in GG-SH infrared spectrum before adsorption, while corresponding absorption peaks of $-CH_2$- appeared at 2920 cm^{-1} after absorption, and the peak intensity decreased, indicating that the alkyl chain participated in self-assembly through intermolecular Van der Waals force. The
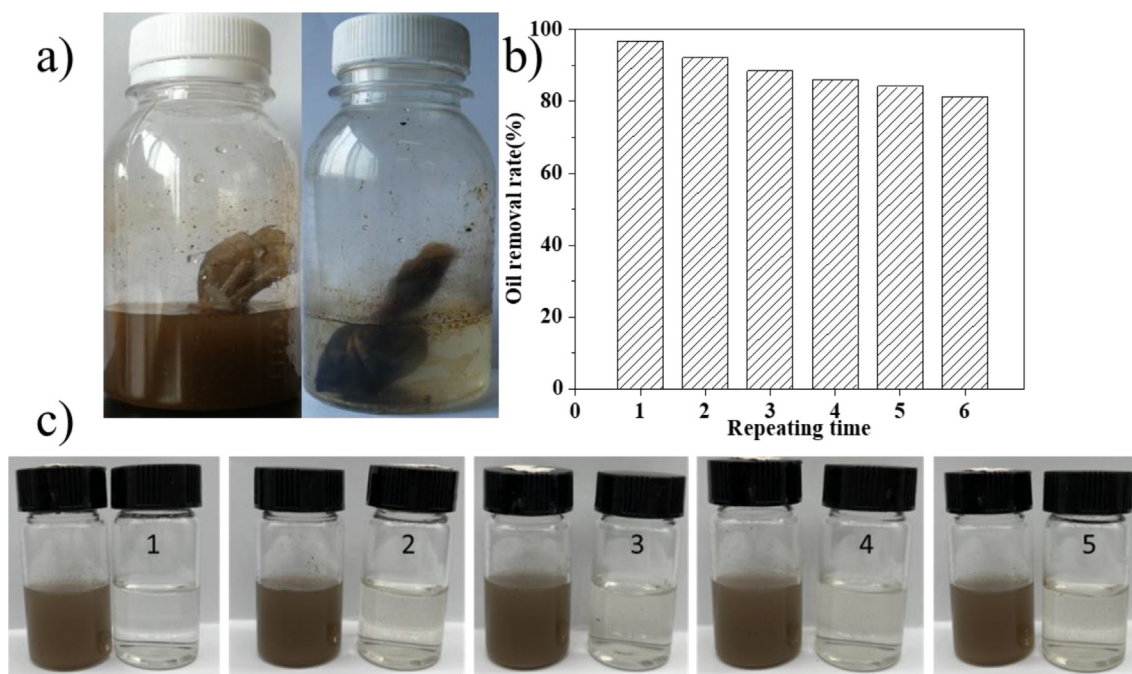

Fig. 8   (a)Oil removal performance of GG-SH package; (b)Change of oil removal rate after recycling experiments (c)Pictures of oily sewage before and after the adsorption treatment in the recycling experiments.
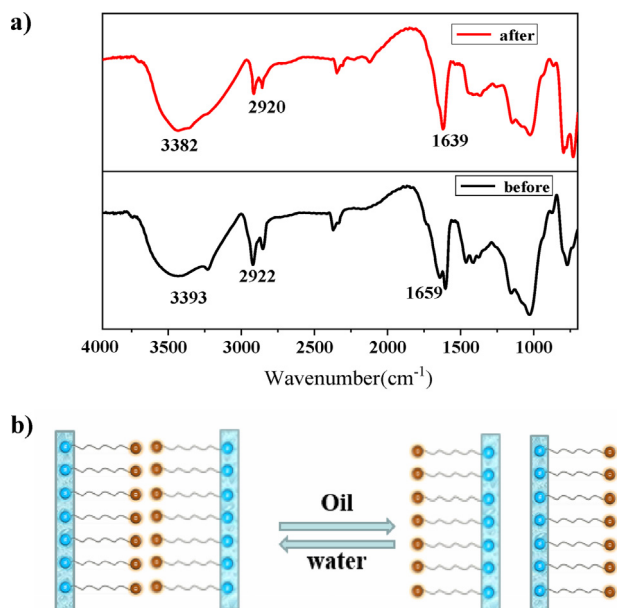
Fig. 9 A)ft-ir spectra of gg-sh before and after adsorption of oily sewage; b) the ''over-turn'' theory of gg-sh in oil–water systems.

above characterization results confirmed that hydrogen bonding between hydrazone groups and polysaccharide hydroxyl groups and van der Waals force of long chain alkyl were the main driving forces of GG-SH oil absorption process.

Furthermore, the ''Over-Turn'' theory is used to explain the process of GG-SH as a hydrophobic modified biological macromolecule material to adsorb oil. In the condensation reaction between hydrazide and aldehyde group, the existence of polar solvent system will lead to a certain degree of hydrophobic repulsion of the hydrophobic groups on the surface of GG-SH, and then hide the non-polar groups in the molecule by virtue of the unidirectional modification of acylhydrazone and the conformational reversal of carbohydrate chain. When there are non-polar components in the system, such as oil droplets in sewage, the alkyl long-chain hydrophobic group will flip out from inside the modified guar gum and appear on the surface of guar gum particles to combine with oil. The hydrophilic action of carbohydrate chain and oilphilic action of long-chain alkyl make oil droplets wrapped in the system, thus completing the adsorption process. Fig. 9b shows the possible mechanism of this process.

4. Conclusion

This paper elaborates the design and application of novel carbohydrate adsorbent based on guar gum functionalized with stearic hydrazide for a simple, ultra-fast, clean and specific treatment towards oily sewage. GG-SH has a good ability to remove crude oil components from aqueous phase by virtue of high specific surface area and strong lipophilicity of long chain alkyl groups. The adsorption isotherms of oil conform to the extended Langmuir equation. Thermodynamic study shows that the oil adsorption on GG-SH is an endothermic spontaneous process. Comparing the IR spectra before and after adsorption, the adsorption mechanism can be concluded that the modified guar gum adsorbed non-polar components through the intermolecular association force between long alkyl chains, indicating that GG-SH is an efficient and renewable polysaccharide-based oil adsorption material and exhibits tremendous potential for sewage treatment and environmental protec-

tion. Although tremendous development in the study of adsorbent has been achieved, there are still plenty of opportunities and challenges remaining in this field. Achieving the following research goals will deepen our comprehension and help to facilitate the creation of environmental material with excellent allround properties. Future work will investigate the use of these low-cost, and low-energy intensive material materials in real wastewater treatment, using effluent mixtures and on a large scale.

Declaration of Competing Interest

The authors declare that they have no known competing financial interests or personal relationships that could have appeared to influence the work reported in this paper.

References

Abdel Maksoud, M.I.A., Elgarahy, A.M., Farrell, C., et al, 2020. Insight on water remediation application using magnetic nanomaterials and biosorbents. Coord. Chem. Rev. 403. https://doi.org/10.1016/j.ccr.2019.213096.

Ahmadi, S.A.R., Kalaee, M.R., Moradi, O., et al, 2021. Core–shell activated carbon-ZIF-8 nanomaterials for the removal of tetracycline from polluted aqueous solution. Adv. Compos. Hybrid Mater. 4, 1384–1397. https://doi.org/10.1007/s42114-021-00357-3.

Ahmadi, S.A.R., Kalaee, M.R., Moradi, O., et al, 2022. Synthesis of novel zeolitic imidazolate framework (ZIF-67) – zinc oxide (ZnO) nanocomposite (ZnO@ZIF-67) and potential adsorption of pharmaceutical (tetracycline (TCC)) from water. J. Mol. Struct. 1251. https://doi.org/10.1016/j.molstruc.2021.132013.

Ahmaruzzaman, M., Gupta, V.K., 2011. Rice husk and its ash as lowcost adsorbents in water and wastewater treatment. Ind. Eng. Chem. Res. 50, 13589–13613. https://doi.org/10.1021/ie201477c.

Al.Haddabi, M., H. Vuthaluru, H. Znad, et al., 2015. Removal of Dissolved Organic Carbon from Oily Produced Water by Adsorption onto Date Seeds: Equilibrium, Kinetic, and Thermodynamic Studies. Water, Air, & Soil Pollution. 226, https://doi.org/10.1007/s11270-015-2443-1.

Alheety, M.A., Raoof, A., Al-Jibori, S.A., et al, 2019. Eco-friendly C60-SESMP-Fe3O4 inorganic magnetizable nanocomposite as high-performance adsorbent for magnetic removal of arsenic from crude oil and water samples. Mater. Chem. Phys. 231, 292–300. https://doi.org/10.1016/j.matchemphys.2019.04.040.

Al-Husaini, I.S., Yusoff, A.R.M., Lau, W.-J., et al, 2019. Iron oxide nanoparticles incorporated polyethersulfone electrospun nanofibrous membranes for effective oil removal. Chem. Eng. Res. Des. 148, 142–154. https://doi.org/10.1016/j.cherd.2019.06.006.

Arabi, M., Ghaedi, M., Ostovan, A., 2016. Development of dummy molecularly imprinted based on functionalized silica nanoparticles for determination of acrylamide in processed food by matrix solid phase dispersion. Food Chem. 210, 78–84. https://doi.org/10.1016/j.foodchem.2016.04.080.

Arabi, M., Ghaedi, M., Ostovan, A., 2017. Water compatible molecularly imprinted nanoparticles as a restricted access material for extraction of hippuric acid, a biological indicator of toluene exposure, from human urine. Microchim. Acta 184, 879–887. https://doi.org/10.1007/s00604-016-2063-5.

Asadu, C.O., Anthony, E.C., Elijah, O.C., et al, 2021. Development of an adsorbent for the remediation of crude oil polluted water using stearic acid grafted coconut husk (Cocos nucifera) composite. Appl. Surf. Sci. Adv. 6. https://doi.org/10.1016/j.apsadv.2021.100179.

Asadu, C.O., Elijah, O.C., Ogbodo, N.O., et al, 2021. Treatment of crude oil polluted water using stearic acid grafted mango seed shell (Mangifera indica) composite. Curr. Res. Green Sustain. Chem. 4. https://doi.org/10.1016/j.crgsc.2021.100169.

Bagheri, A.R., Arabi, M., Ghaedi, M., et al, 2019. Dummy molecularly imprinted polymers based on a green synthesis strategy for magnetic solid-phase extraction of acrylamide in food samples. Talanta 195, 390–400. https://doi.org/10.1016/j.talanta.2018.11.065.

Bai, B., Bai, F., Li, X., et al, 2022. The remediation efficiency of heavy metal pollutants in water by industrial red mud particle waste. Environ. Technol. Innov. 28. https://doi.org/10.1016/j.eti.2022.102944.

Bajpai, S.K., Chanpuria, A., Dubey, S., 2020. Magnetically driven poly(sulfur/oil) composite as an efficient oil adsorbent. part-I: synthesis, characterization and preliminary oil removal study. Environ. Nanotechnol. Monit. Manage. 13. https://doi.org/10.1016/j.enmm.2020.100293.

Baloo, L., Isa, M.H., Sapari, N.B., et al, 2021. Adsorptive removal of methylene blue and acid orange 10 dyes from aqueous solutions using oil palm wastes-derived activated carbons. Alex. Eng. J. 60, 5611–5629. https://doi.org/10.1016/j.aej.2021.04.044.

Bao, Y., Zhou, Q., Zhang, M., et al, 2019. Wet-spun nanoTiO2/chitosan nanocomposite fibers as efficient and retrievable absorbent for the removal of free fatty acids from edible oil. Carbohydr. Polym. 210, 119–126. https://doi.org/10.1016/j.carbpol.2019.01.035.

Bi, J., Huang, X., Wang, J., et al, 2019. Oil-phase cyclic magnetic adsorption to synthesize Fe3O4@C@TiO2-nanotube composites for simultaneous removal of Pb(II) and Rhodamine B. Chem. Eng. J. 366, 50–61. https://doi.org/10.1016/j.cej.2019.02.017.

Black, T.A., White, M.S., Blais, J.M., et al, 2021. Surface oil is the primary driver of macroinvertebrate impacts following spills of diluted bitumen in freshwater. Environ. Pollut. 290,. https://doi.org/10.1016/j.envpol.2021.117929 117929.

Chai, W., Liu, X., Zou, J., et al, 2015. Pomelo peel modified with acetic anhydride and styrene as new sorbents for removal of oil pollution. Carbohydr. Polym. 132, 245–251. https://doi.org/10.1016/j.carbpol.2015.06.060.

Chandrika, K.P., Singh, A., Rathore, A., et al, 2016. Novel cross linked guar gum-g-poly(acrylate) porous superabsorbent hydrogels: characterization and swelling behaviour in different environments. Carbohydr. Polym. 149, 175–185. https://doi.org/10.1016/j.carbpol.2016.04.077.

Cheng, H., Li, Z., Li, Y., et al, 2020. Multi-functional magnetic bacteria as efficient and economical Pickering emulsifiers for encapsulation and removal of oil from water. J. Colloid Interface Sci. 560, 349–358. https://doi.org/10.1016/j.jcis.2019.10.045.

Chhabra, A. and K. Singh, 2021. Engine oil dialysis of heavy-duty engine oil 5W50. Materials Today: Proceedings. https://doi.org/10.1016/j.matpr.2021.12.156.

Damavandi, F., Soares, J.B.P., 2022. Polystyrene magnetic nanocomposite blend: an effective, facile, and economical alternative in oil spill removal applications. Chemosphere 286. https://doi.org/10.1016/j.chemosphere.2021.131611.

Ding, L., Song, J., Huang, D., et al, 2021. Simultaneous removal of nitrate and hexavalent chromium in groundwater using indigenous microorganisms enhanced by emulsified vegetable oil: interactions

and remediation threshold values. J. Hazard. Mater. 406. https://doi.org/10.1016/j.jhazmat.2020.124708.

Diraki, A., Mackey, H.R., McKay, G., et al, 2019. Removal of emulsified and dissolved diesel oil from high salinity wastewater by adsorption onto graphene oxide. J. Environ. Chem. Eng. 7. https://doi.org/10.1016/j.jece.2019.103106.

Duan, M., Ma, J., Fang, S., 2019. Synthesis of hydrazine-grafted guar gum material for the highly effective removal of organic dyes. Carbohydr. Polym. 211, 308–314. https://doi.org/10.1016/j.carbpol.2019.01.112.

El Assimi, T., Roko, B., El Kadib, A., et al, 2019. Synthesis of poly (epsilon-caprolactone)-grafted guar gum by surface-initiated ring-opening polymerization. Carbohydr. Polym. 220, 95–102. https://doi.org/10.1016/j.carbpol.2019.05.049.

El Shahawy, A., Heikal, G., 2018. Organic pollutants removal from oily wastewater using clean technology economically, friendly biosorbent (Phragmites australis). Ecol. Eng. 122, 207–218. https://doi.org/10.1016/j.ecoleng.2018.08.004.

El-Maghrabi, H.H., Hosny, R., Ramzi, M., et al, 2019. Preparation and characterization of novel magnetic ZnFe2O4–hydroxyapatite core-shell nanocomposite and its use as fixed bed column system for removal of oil residue in oily wastewater samples. Egypt. J. Pet. 28, 137–144. https://doi.org/10.1016/j.ejpe.2018.12.005.

Elmobarak, W.F., Almomani, F., 2021. Application of magnetic nanoparticles for the removal of oil from oil-in-water emulsion: regeneration/reuse of spent particles. J. Pet. Sci. Eng. 203. https://doi.org/10.1016/j.petrol.2021.108591.

Elmobarak, W.F., Almomani, F., 2021. Enhanced oil recovery using hyperbranched polyglycerol polymer-coated silica nanoparticles. Chemosphere 285,. https://doi.org/10.1016/j.chemosphere.2021.131295 131295.

Farahbod, F., Afkhami Karaei, M., 2021. Mathematical modeling and experimental study of sulfur removal process from light and heavy crude oil in a bed occupied by ferric oxide nanocatalysts. Environ. Technol. Innov. 23. https://doi.org/10.1016/j.eti.2021.101656.

Ge, D., Yuan, H., Xiao, J., et al, 2019. Insight into the enhanced sludge dewaterability by tannic acid conditioning and pH regulation. Sci. Total Environ. 679, 298–306. https://doi.org/10.1016/j.scitotenv.2019.05.060.

Gihar, S., Kumar, D., Kumar, P., 2021. Facile synthesis of novel pH-sensitive grafted guar gum for effective removal of mercury (II) ions from aqueous solution. Carbohydr. Polym. Technol. Appl. 2. https://doi.org/10.1016/j.carpta.2021.100110.

Gkogkou, D., Rizogianni, S., Tziasiou, C., et al, 2021. Highly efficient removal of crude oil and dissolved hydrocarbons from water using superhydrophobic cotton filters. J. Environ. Chem. Eng. 9. https://doi.org/10.1016/j.jece.2021.106170.

Guan, Q., Zeng, G., Song, J., et al, 2021. Ultrasonic power combined with seed materials for recovery of phosphorus from swine wastewater via struvite crystallization process. J. Environ. Manage. 293,. https://doi.org/10.1016/j.jenvman.2021.112961 112961.

Gupta, V.K., Nayak, A., Agarwal, S., et al, 2014. Potential of activated carbon from waste rubber tire for the adsorption of phenolics: effect of pre-treatment conditions. J. Colloid Interface Sci. 417, 420–430. https://doi.org/10.1016/j.jcis.2013.11.067.

Gurav, R., Bhatia, S.K., Choi, T.-R., et al, 2021. Adsorptive removal of crude petroleum oil from water using floating pinewood biochar decorated with coconut oil-derived fatty acids. Sci. Total Environ. 781. https://doi.org/10.1016/j.scitotenv.2021.146636.

Guselnikova, O., Semyonov, O., Kirgina, M., et al, 2021. Polymer waste surgical masks decorated by superhydrophobic metal-organic frameworks towards oil spills clean-up. J. Environ. Chem. Eng. https://doi.org/10.1016/j.jece.2021.107105.

Haselroth, K.J., Wilke, P., Dalla Costa, I.M., et al, 2021. Effectiveness of Aeromonas hydrophila for the removal of oil and grease from cattle slaughterhouse effluent. J. Clean. Prod. 287. https://doi.org/10.1016/j.jclepro.2020.125533.

He, H., Zhang, T.C., Ouyang, L., et al, 2022. Superwetting and photocatalytic Ag2O/TiO2@CuC2O4 nanocomposite-coated mesh membranes for oil/water separation and soluble dye removal. Mater. Today Chem. 23. https://doi.org/10.1016/j.mtchem.2021.100717.

Javadian, S., M. khalilifard and S. M. Sadrpoor, 2019. Functionalized graphene oxide with core-shell of Fe3O4@oliec acid nanospheres as a recyclable demulsifier for effective removal of emulsified oil from oily wastewater. Journal of Water Process Engineering. 32, https://doi.org/10.1016/j.jwpe.2019.100961.

Jiat Lee, X., B. Yan Zhang Hiew, K. Chiew Lai, et al., 2021. Evaluation of industrial palm oil sludge as an effective green adsorbing substrate for toxic aqueous cadmium removal. Materials Science for Energy Technologies. 4, 224-235. https://doi.org/10.1016/j.mset.2021.06.002.

Kallem, P., Othman, I., Ouda, M., et al, 2021. Polyethersulfone hybrid ultrafiltration membranes fabricated with polydopamine modified ZnFe2O4 nanocomposites: applications in humic acid removal and oil/water emulsion separation. Process Saf. Environ. Prot. 148, 813–824. https://doi.org/10.1016/j.psep.2021.02.002.

Kilany, A.Y., Nosier, S.A., Hussein, M., et al, 2020. Combined oil demulsification and copper removal from copper plating plant effluents by electrocoagulation in a new cell design. Sep. Purif. Technol. 248. https://doi.org/10.1016/j.seppur.2020.117056.

Kirkebæk, B., Simoni, G., Lankveld, I., et al, 2021. Oleic acid-coated magnetic particles for removal of oil from produced water. J. Pet. Sci. Eng. https://doi.org/10.1016/j.petrol.2021.110088.

Krebsz, M., Pasinszki, T., Tung, T.T., et al, 2021. Multiple applications of bio-graphene foam for efficient chromate ion removal and oil-water separation. Chemosphere 263,. https://doi.org/10.1016/j.chemosphere.2020.127790 127790.

Lawal, A.A., Hassan, M.A., Ahmad Farid, M.A., et al, 2021. Adsorption mechanism and effectiveness of phenol and tannic acid removal by biochar produced from oil palm frond using steam pyrolysis. Environ. Pollut. 269,. https://doi.org/10.1016/j.envpol.2020.116197 116197.

Li, X., Han, D., Zhang, M., et al, 2019. Removal of toxic dyes from aqueous solution using new activated carbon materials developed from oil sludge waste. Colloids Surf. A Physicochem. Eng. Asp. 578. https://doi.org/10.1016/j.colsurfa.2019.05.066.

Li, L., Rong, L., Xu, Z., et al, 2020. Cellulosic sponges with pH responsive wettability for efficient oil-water separation. Carbohydr. Polym. 237,. https://doi.org/10.1016/j.carbpol.2020.116133 116133.

Li, Y., Wang, M., Sun, D., et al, 2018. Effective removal of emulsified oil from oily wastewater using surfactant-modified sepiolite. Appl. Clay Sci. 157, 227–236. https://doi.org/10.1016/j.clay.2018.02.014.

Li, W., Xie, Z., Xue, S., et al, 2021. Studies on the adsorption of dyes, Methylene blue, Safranin T, and Malachite green onto Polystyrene foam. Sep. Purif. Technol. 276. https://doi.org/10.1016/j.seppur.2021.119435.

Liu, J., Liu, G., Liu, W., 2014. Preparation of water-soluble β-cyclodextrin/poly(acrylic acid)/graphene oxide nanocomposites as new adsorbents to remove cationic dyes from aqueous solutions. Chem. Eng. J. 257, 299–308. https://doi.org/10.1016/j.cej.2014.07.021.

Liu, J., Qu, X., Zhang, C., et al, 2022. High-yield aqueous synthesis of partial-oxidized black phosphorus as layered nanodot photocatalysts for efficient visible-light driven degradation of emerging organic contaminants. J. Clean. Prod. 377. https://doi.org/10.1016/j.jclepro.2022.134228.

Liu, M., Xie, Z., Ye, H., et al, 2021. Waste polystyrene foam – Chitosan composite materials as high-efficient scavenger for the anionic dyes. Colloids Surf. A Physicochem. Eng. Asp. 627. https://doi.org/10.1016/j.colsurfa.2021.127155.

Liu, W., Zheng, J., Ou, X., et al, 2018. Effective extraction of Cr(VI) from hazardous gypsum sludge via controlling the phase transformation and chromium species. Environ. Sci. Technol. 52, 13336–13342. https://doi.org/10.1021/acs.est.8b02213.

Ma, J., Fang, S., Shi, P., et al, 2019. Hydrazine-Functionalized guar-gum material capable of capturing heavy metal ions. Carbohydr. Polym. 223,. https://doi.org/10.1016/j.carbpol.2019.115137 115137.

Magalhães, E.R.B., Fonseca de Menezes, N.N., Silva, F.L., et al, 2021. Effect of oil extraction on the composition, structure, and coagulant effect of Moringa oleifera seeds. J. Clean. Prod. 279. https://doi.org/10.1016/j.jclepro.2020.123902.

Mahdi, W.A., Hussain, A., Bukhari, S.I., et al, 2021. Removal of clarithromycin from aqueous solution using water/triton X-100/ ethanol/ olive oil green nanoemulsion method. J. Water Process Eng. 40. https://doi.org/10.1016/j.jwpe.2021.101973.

Martins, D., Estevinho, B., Rocha, F., et al, 2020. A dry and fully dispersible bacterial cellulose formulation as a stabilizer for oil-in-water emulsions. Carbohydr. Polym. 230,. https://doi.org/10.1016/j.carbpol.2019.115657 115657.

Medina, O.E., Galeano-Caro, D., Castelo-Quibén, J., et al, 2021. Monolithic carbon xerogels-metal composites for crude oil removal from oil in-saltwater emulsions and subsequent regeneration through oxidation process: Composites synthesis, adsorption studies, and oil decomposition experiments. Micropor. Mesopor. Mater. 319. https://doi.org/10.1016/j.micromeso.2021.111039.

Mottaghi, H., Mohammadi, Z., Abbasi, M., et al, 2021. Experimental investigation of crude oil removal from water using polymer adsorbent. J. Water Process Eng. 40. https://doi.org/10.1016/j.jwpe.2021.101959.

Mukherjee, S., Mukhopadhyay, S., Zafri, M.Z.B., et al, 2018. Application of guar gum for the removal of dissolved lead from wastewater. Ind. Crop. Prod. 111, 261–269. https://doi.org/10.1016/j.indcrop.2017.10.022.

Naeini, A.H., Kalaee, M., Moradi, O., et al, 2022. Eco-friendly inorganic-organic bionanocomposite (Copper oxide — Carboxyl methyl cellulose — Guar gum): preparation and effective removal of dye from aqueous solution. Korean J. Chem. Eng. 39, 2138–2147. https://doi.org/10.1007/s11814-022-1074-7.

Naeini, A.H., Kalaee, M.R., Moradi, O., et al, 2022. Synthesis, characterization and application of Carboxylmethyl cellulose, Guar gam, and Graphene oxide as novel composite adsorbents for removal of malachite green from aqueous solution. Adv. Compos. Hybrid Mater. 5, 335–349. https://doi.org/10.1007/s42114-021-00388-w.

Osman, A.I., Elgarahy, A.M., Mehta, N., et al, 2022. Facile synthesis and life cycle assessment of highly active magnetic sorbent composite derived from mixed plastic and biomass waste for water remediation. ACS Sustain. Chem. Eng. 10, 12433–12447. https://doi.org/10.1021/acssuschemeng.2c04095.

Ostovan, A., Ghaedi, M., Arabi, M., 2018. Fabrication of water-compatible superparamagnetic molecularly imprinted biopolymer for clean separation of baclofen from bio-fluid samples: a mild and green approach. Talanta 179, 760–768. https://doi.org/10.1016/j.talanta.2017.12.017.

Patra, A.S., Ghorai, S., Sarkar, D., et al, 2017. Anionically functionalized guar gum embedded with silica nanoparticles: An efficient nanocomposite adsorbent for rapid adsorptive removal of toxic cationic dyes and metal ions. Bioresour. Technol. 225, 367–376. https://doi.org/10.1016/j.biortech.2016.11.093.

Phanthong, P., Reubroycharoen, P., Kongparakul, S., et al, 2018. Fabrication and evaluation of nanocellulose sponge for oil/water separation. Carbohydr. Polym. 190, 184–189. https://doi.org/10.1016/j.carbpol.2018.02.066.

Sakti, S.C.W., Wijaya, R.A., Indrasari, N., et al, 2021. Magnetic hollow buoyant alginate beads achieving rapid remediation of oil contamination on water. J. Environ. Chem. Eng. 9. https://doi.org/10.1016/j.jece.2020.104935.

Sakti, S.C.W., Indrasari, N., Wijaya, R.A., et al, 2022. Diatomaceous earth incorporated floating magnetic beads for oil removal on water. Environ. Technol. Innov. 25. https://doi.org/10.1016/j.eti.2021.102120.

Saya, L., Malik, V., Singh, A., et al, 2021. Guar gum based nanocomposites: role in water purification through efficient removal of dyes and metal ions. Carbohydr. Polym. 261,. https://doi.org/10.1016/j.carbpol.2021.117851 117851.

Schaefer, S., Gadonneix, P., Celzard, A., et al, 2021. Carbon gels derived from phenolic-oil for pollutants removal in water phase. Fuel Process. Technol. 211. https://doi.org/10.1016/j.fuproc.2020.106588.

Shamloufard, A., Hajati, S., Youzbashi, A.A., et al, 2022. S-scheme NIR-edge Ag3CuS2/VO2 heterostructure for photo-oxidation/reduction of methylene blue/Cr (VI). Appl. Surf. Sci. 590. https://doi.org/10.1016/j.apsusc.2022.153118.

Shi, Y., Cheng, X., Wan, D., et al, 2021. Construction of the micro-electrolysis system by Fe0 and clay-carbon derived from oil refining for the removal of ozone disinfection by-products. Colloids Surf. A Physicochem. Eng. Asp. https://doi.org/10.1016/j.colsurfa.2021.128224.

Shi, T., Xie, Z., Zhu, Z., et al, 2022. Effective removal of metal ions and cationic dyes from aqueous solution using different hydrazine-dopamine modified sodium alginate. Int. J. Biol. Macromol. 195, 317–328. https://doi.org/10.1016/j.ijbiomac.2021.12.039.

Shui, T., Pan, M., Lu, Y., et al, 2021. High-efficiency and durable removal of water-in-heavy oil emulsions enabled by delignified and carboxylated basswood with zwitterionic nanohydrogel coatings. J. Colloid Interface Sci. https://doi.org/10.1016/j.jcis.2021.12.146.

Sun, G.Z., Chen, X.G., Li, Y.Y., et al, 2008. Preparation and properties of amphiphilic chitosan derivative as a coagulation agent. Environ. Eng. Sci. 25, 1325–1332. https://doi.org/10.1089/ees.2007.0329.

Tabatabaeian, R., Dinari, M., Aliabadi, H.M., 2021. Cross-linked bionanocomposites of hydrolyzed guar gum/magnetic layered double hydroxide as an effective sorbent for methylene blue removal. Carbohydr. Polym. 257,. https://doi.org/10.1016/j.carbpol.2021.117628 117628.

Tan, Z., Zhu, H., He, X., et al, 2022. Effect of ventilation quantity on electron transfer capacity and spectral characteristics of humic substances during sludge composting. Environ. Sci. Pollut. Res. Int. 29, 70269–70284. https://doi.org/10.1007/s11356-022-20808-8.

Tang, X., Wu, J., Wu, W., et al, 2020. Competitive-type pressure-dependent immunosensor for highly sensitive detection of diace-toxyscirpenol in wheat via monoclonal antibody. Anal. Chem. 92, 3563–3571. https://doi.org/10.1021/acs.analchem.9b03933.

Tawfik, A., Alalm, M.G., Awad, H.M., et al, 2022. Solar photo-oxidation of recalcitrant industrial wastewater: a review. Environ. Chem. Lett. 20, 1839–1862. https://doi.org/10.1007/s10311-022-01390-4.

Wang, B., Dai, L., Yang, G., et al, 2019. A highly efficient thermo responsive palladium nanoparticles incorporated guar gum hydro-gel for effective catalytic reactions. Carbohydr. Polym. 226,. https://doi.org/10.1016/j.carbpol.2019.115289 115289.

Wang, Y., Wu, X., Liu, J., et al, 2022. Mo-modified band structure and enhanced photocatalytic properties of tin oxide quantum dots for visible-light driven degradation of antibiotic contaminants. J. Environ. Chem. Eng. 10. https://doi.org/10.1016/j.jece.2021.107091.

Wen, Y., Xie, Z., Xue, S., et al, 2021. Functionalized polymethyl methacrylate-modified dialdehyde guar gum containing hydrazide groups for effective removal and enrichment of dyes, ion, and oil/water separation. J. Hazard. Mater. https://doi.org/10.1016/j.jhazmat.2021.127799.

Wu, M., Zhai, M., Li, X., 2021. Adsorptive removal of oil drops from ASP flooding-produced water by polyether polysiloxane-grafted ZIF-8. Powder Technol. 378, 76–84. https://doi.org/10.1016/j.powtec.2020.09.068.

Yamini, Y., Ghambarian, M., Esrafili, A., et al, 2012. Rapid determination of ultra-trace amounts of acrylamide contaminant in water samples using dispersive liquid–liquid microextraction coupled to gas chromatography-electron capture detector. Int. J. Environ. Anal. Chem. 92, 1493–1505. https://doi.org/10.1080/03067319.2010.548098.

Yang, Y., Chen, F., Chen, Q., et al, 2017. Synthesis and character-ization of grafting polystyrene from guar gum using atom transfer radical addition. Carbohydr. Polym. 176, 266–272. https://doi.org/10.1016/j.carbpol.2017.08.081.

Yang, K., Ren, J., Cui, Y., et al, 2021. Fabrication of porous tubular carbon fibers from the fruits of Platanus orientalis and their high oil adsorption properties. J. Environ. Chem. Eng. 9. https://doi.org/10.1016/j.jece.2021.105706.

Yang, S., Wang, F., Tang, Q., et al, 2019. Utilization of ultra-light carbon foams for the purification of emulsified oil wastewater and their adsorption kinetics. Chem. Phys. 516, 139–146. https://doi.org/10.1016/j.chemphys.2018.08.051.

Zhang, Y.R., Chen, J.T., Hao, B., et al, 2020. Preparation of cellulose-coated cotton fabric and its application for the separation of emulsified oil in water. Carbohydr. Polym. 240,. https://doi.org/10.1016/j.carbpol.2020.116318 116318.

Zhang, J., Li, H., Mei, D., et al, 2021. Steamed bun-derived microporous carbon for oil-water separation. Colloids Surf. A Physicochem. Eng. Asp. 629. https://doi.org/10.1016/j.colsurfa.2021.127389.

Zhang, X., Wang, B., Wang, B., et al, 2021. Superhydrophobic cellulose acetate/multiwalled carbon nanotube monolith with fiber cluster network for selective oil/water separation. Carbohydr. Polym. 259,. https://doi.org/10.1016/j.carbpol.2021.117750 117750.